Multi-Stream Transmission in Massive MIMO Systems With Full-Duplex Bi-Directional Communication Links

Bridget Durowaa Antwi-Boasiako, Prince Anokye, Derek Kwaku Pobi Asiedu, Roger Kwao Ahiadormey, Kyoung-Jae Lee, Andreas F Molisch

This article has been accepted for publication in IEEE Transactions on Vehicular Technology. This is the author's version which has not been fully edited and content may change prior to final publication. Citation information: DOI 10.1109/TVT.2023.3266715

Multi-Stream Transmission in Massive MIMO Systems with Full-Duplex Bi-Directional Communication Links

Bridget Durowaa Antwi-Boasiako, Prince Anokye, Derek Kwaku Pobi Asiedu, Roger Kwao Ahiadormey, Kyoung-Jae Lee, *Senior Member, IEEE*, and Andreas F. Molisch, *Fellow, IEEE*

***Abstract*—This paper considers a full-duplex (FD) multi-user massive multiple-input multiple-output system where the base station (BS) and user equipment (UE) bi-directionally transmit and receive multiple independent data streams over the same frequency band. The BS and UEs are equipped with a large-scale antenna array. Accounting for imperfect channel state information, we derive the closed-form expressions for the achievable sum-rate and sum spectral efficiency (SE) for the proposed model using maximum-ratio combining and zero-forcing detection. The analytical solutions are verified with simulations. In addition, our analytical results highlight the benefits of multi-stream transmission and show an improved SE for fewer UEs. Moreover, the results show that increasing the antenna array size helps combat self-interference.**

***Index Terms*—Full-duplex, massive multiple-input multiple-output, maximum-ratio combining, zero-forcing.**

I. Introduction

With the focus of research geared towards fifth-generation and beyond wireless systems, enabling technologies such as massive multiple-input multiple-output (mMIMO) and full-duplex (FD) communications have been proposed [1]–[3]. In mMIMO, the base station (BS) is equipped with a large array of antennas to serve multiple users. The massive antennas reduce signal interference and offer high data rates due to the large-scale diversity and multiplexing gain [1], [4]. Many existing works focus on the performance of mMIMO systems with single-antenna user equipment (UEs) [1], [5]. In [1], the authors analyze a multi-user mMIMO system and derive the uplink (UL) spectral efficiency (SE) with both perfect and imperfect channel state information (CSI). To detect the transmitted signals, [1] exploits detection schemes like maximum-ratio combining (MRC), zero-forcing (ZF), and minimum mean-square error (MMSE). Similarly, [5] acquires imperfect CSI using a proposed beamforming training scheme and derives the achievable downlink (DL) rate of a multi-user mMIMO system. Although [1] and [5] only consider single-antenna UEs, many modern UEs like tablets and smart vehicles are able to support multiple or large antenna arrays [6]. The authors of [4] show that with the additional UE antennas, multiple data streams can be multiplexed per user, thereby increasing the multiplexing gain and SE. The BSs and UEs in [1], [4], and [5] operate in a half-duplex (HD) mode. However, it has been shown that transmitting and receiving data simultaneously on the same time-frequency resources, also known as full-duplex (FD) operation, has the potential to double the SE relative to the HD mode [7], [8]. Thus, the work in [9] investigates an FD distributed massive MIMO system with single-antenna HD UL and DL users and optimizes the antenna selection vector to maximize the achievable rate. Also, the authors of [10] consider a separate-antenna FD BS serving HD multi-antenna UEs and explore the antenna ratio to maximize the sum-rate. The FD transceiver can alternatively have a single antenna design. Either design of FD reduces the leakage of antenna signals from the transmitter to its receiver, referred to as self-interference (SI). Apart from the natural isolation provided by the FD antenna configuration, time-domain cancellation and spatial suppression schemes can also be used to mitigate the SI [2]. For an FD BS and FD UEs with a single transmit/receive antenna, the work [8] derives the UL/DL SE by adopting ZF while [7] investigates the asymptotic sum-rate for a ZF-based FD mMIMO relaying system with separate multi-antenna FD MIMO UEs. The UEs in [7] and [8] are however, equipped with only a few antennas and both works assume perfect CSI.

Given the advantages of large-scale arrays, which include providing a high degree of freedom (DoF) for information transmission, there is a need to study the performance of large-scale antenna UEs in separate-antenna FD mMIMO systems. In particular, this work investigates a mMIMO system consisting of an FD BS and FD-enabled UEs assuming imperfect CSI. The main contributions of this work are summarized below:

- We derive closed-form lower bound[1] solutions for the sum-rate with multiple data stream transmission using MRC and ZF. The closed-form solutions are shown to be tight relative to the simulation results.
- We also investigate the impact of multiple data stream transmission on the sum SE. The sum SE initially increases with the number of streams. However, further increase in data streams causes the sum SE to deteriorate.
- Furthermore, we compare the SE of the mMIMO system in FD and HD modes and characterize the impact of the residual SI on the performance.

Notation: Lowercase and uppercase boldface letters denote vectors and matrices, respectively. The notation $(\cdot)^H$ is the Hermitian transpose. $\mathbb{E}\{\cdot\}$ is the expectation of a random variable, while $\mathcal{CN}(0,\sigma^2)$ denotes circularly complex Gaussian distribution with zero mean and variance σ^2. $(\cdot)^b$ and $(\cdot)^s$ are variables related to the BS and UEs, respectively.

II. System Model

This work considers a mMIMO system where an FD BS and K FD UEs communicate simultaneously via bi-directional links, as shown in Fig. 1. We assume a block fading model where the channels remain constant within a coherence interval T, but vary independently from block to block. Each UE has N_T (multiple) transmit and N_R (massive) receive antennas, such that $N_R \gg N_T$. The l-th UE transmits $N_S \leq N_T$ independent data streams to the BS, $\forall l = 1, \cdots, K$. Similarly, the BS has M_T (multiple) transmit and M_R (massive) receive antennas, such that $M_R \gg M_T$. Without loss of generality, we assume that the BS allocates M_S antennas[2] to transmit M_S independent data streams (i.e., one stream per antenna) to each UE such that the lth group of antennas at the BS transmits M_S streams to the l-th UE and $KM_S \leq M_T$. Also, $M_R \gg KN_S$ and $N_R \gg M_S$ [12]. The BS and UEs suffer multi-stream interference since they transmit multiple independent data streams. Due to FD capability, all the nodes also experience SI. UE-to-UE interference also occurs since all K UEs transmit and receive data on the same frequency. Let us define the UL channel from the l-th UE to the BS as $\mathbf{H}_l = [\mathbf{h}_{l,1}, \mathbf{h}_{l,2}, \cdots, \mathbf{h}_{l,N_S}] \in \mathbb{C}^{M_R \times N_S}$ where $\mathbf{h}_{l,n}$ is the n-th column of $\mathbf{H}_l$, $\forall n = 1, \cdots, N_S$ and $\mathbf{H} = [\mathbf{H}_1, \mathbf{H}_2, \cdots, \mathbf{H}_K] \in \mathbb{C}^{M_R \times KN_S}$. Let $\mathbf{G}_{ll} = [\mathbf{g}_{ll,1}, \cdots, \mathbf{g}_{ll,2}, \cdots, \mathbf{g}_{ll,M_S}] \in \mathbb{C}^{N_R \times M_S}$ be the DL channel from the l-th group of antennas at the BS to the l-th UE

B. D. A.-Boasiako, P. Anokye, and K.-J. Lee are with the Department of Electronic Engineering, Hanbat National University, Daejeon 34158, Republic of Korea (e-mail: brigantwi@gmail.com; princemcanokye@yahoo.com; kyoungjae@hanbat.ac.kr)

D. K. P. Asiedu and R. K. Ahiadormey are with the Communications Division, Council for Scientific and Industrial Research–Institute for Scientific and Technological Information (CSIR-INSTI), Accra, Ghana (e-mail: kwakupobi@gmail.com; rogerkwao@gmail.com)

A. F. Molisch is with the Ming Hsieh Department of Electrical and Computer Engineering, University of Southern California, Los Angeles, CA, 90089 USA (e-mail: molisch@usc.edu).

Corresponding author: K.-J. Lee.

[1]By employing the bounding technique in [2], [3], a lower bound on the achievable sum-rate can be obtained.

[2]We assume that the antennas are separated by 5-10 wavelength [11].

This article has been accepted for publication in IEEE Transactions on Vehicular Technology. This is the author's version which has not been fully edited and content may change prior to final publication. Citation information: DOI 10.1109/TVT.2023.3266715

where $\mathbf{g}_{ll,m}$ is the m-th column of $\mathbf{G}_{ll}$, $\forall m = 1, \cdots, M_S$ and $\mathbf{G}_l = [\mathbf{G}_{l1}, \cdots, \mathbf{G}_{ll}, \cdots \mathbf{G}_{lk'}, \cdots, \mathbf{G}_{lK}] \in \mathbb{C}^{N_R \times KM_S}$, $\forall k' \neq l$. $\mathbf{H}_l$ and $\mathbf{G}_{ll}$ are expressed as $\mathbf{H}_l = \bar{\mathbf{H}}_l \dot{\mathbf{D}}_l^{\frac{1}{2}}$ and $\mathbf{G}_{ll} = \bar{\mathbf{G}}_{ll} \ddot{\mathbf{D}}_{ll}^{\frac{1}{2}}$, respectively, where $\bar{\mathbf{H}}_l$ and $\bar{\mathbf{G}}_{ll}$ are the small-scale fading matrices. $\dot{\mathbf{D}}_l$ and $\ddot{\mathbf{D}}_{ll}$ are the diagonal matrices of the large-scale fading coefficients with n-th element $\beta_{l,n}$ and m-th element $\beta_{ll,m}$, respectively. $\dot{\mathbf{D}}_l$ and $\ddot{\mathbf{D}}_{ll}$ describe the geometric pathloss and shadowing and are assumed to be known a-priori [1]. The channels are assumed to undergo independent and identically distributed (i.i.d.) Rayleigh fading due to the rich scattering environment [2], [12].

A. Channel Estimation

For each coherence interval T, the channels are estimated via UL training for a duration τ_p while the remaining timeslot, i.e., $T - \tau_p$ is used for data transmission. All K UEs transmit pilot symbols to the BS. Simultaneously, the BS sends pilots to each UE[3]. Here, we adopt the linear MMSE-based channel estimation. Thus the true channel matrices $\mathbf{H}$ and $\mathbf{G}_l$ are decomposed as [3] $\mathbf{H} = \hat{\mathbf{H}} + \tilde{\mathbf{H}}, \mathbf{G}_l = \hat{\mathbf{G}}_l + \tilde{\mathbf{G}}_l$, where $\hat{\mathbf{H}} = [\hat{\mathbf{H}}_1, \hat{\mathbf{H}}_2, \cdots, \hat{\mathbf{H}}_K] \in \mathbb{C}^{M_R \times KN_S}$ and $\tilde{\mathbf{H}} = [\tilde{\mathbf{H}}_1, \tilde{\mathbf{H}}_2, \cdots, \tilde{\mathbf{H}}_K] \in \mathbb{C}^{M_R \times KN_S}$ indicate the UL channel estimate and the estimation error matrices, respectively. $\hat{\mathbf{G}}_l \in \mathbb{C}^{N_R \times KM_S}$ and $\tilde{\mathbf{G}}_l \in \mathbb{C}^{N_R \times KM_S}$ represent the DL channel estimates and the estimation error matrices from the BS to the l-th UE, respectively. Due to the orthogonality property of the MMSE estimation, the channel estimates and estimation error matrices are mutually independent [2]. Also, $\mathbf{h}_{l,n}$ and $\mathbf{g}_{ll,m}$ are written, respectively, as $\mathbf{h}_{l,n} = \hat{\mathbf{h}}_{l,n} + \tilde{\mathbf{h}}_{l,n}$ and $\mathbf{g}_{ll,m} = \hat{\mathbf{g}}_{ll,m} + \tilde{\mathbf{g}}_{ll,m}$. $\hat{\mathbf{h}}_{l,n} \sim \mathcal{CN}(\mathbf{0}, \hat{\beta}^2_{l,n}\mathbf{I}_{M_R})$, $\tilde{\mathbf{h}}_{l,n} \sim \mathcal{CN}(\mathbf{0}, \tilde{\beta}^2_{l,n}\mathbf{I}_{M_R})$ denote the n-th columns of $\hat{\mathbf{H}}_l$ and $\tilde{\mathbf{H}}_l$ (i.e. the l-th columns of $\hat{\mathbf{H}}$ and $\tilde{\mathbf{H}}$), respectively. Similarly, $\hat{\mathbf{g}}_{ll,m} \sim \mathcal{CN}(\mathbf{0}, \hat{\beta}^2_{ll,m}\mathbf{I}_{N_R})$ and $\tilde{\mathbf{g}}_{ll,m} \sim \mathcal{CN}(\mathbf{0}, \tilde{\beta}^2_{ll,m}\mathbf{I}_{N_R})$ are defined as the m-th columns of $\hat{\mathbf{G}}_{ll}$ and $\tilde{\mathbf{G}}_{ll}$, respectively. $\hat{\beta}^2_{l,n}$ and $\hat{\beta}^2_{ll,m}$ denote the variances of $\hat{\mathbf{h}}_{l,n}$ and $\hat{\mathbf{g}}_{ll,m}$ given, respectively, as $\hat{\beta}^2_{l,n} \triangleq \frac{p_p \tau_p \beta^2_{l,n}}{\tau_p p_p \beta_{l,n}+1}$ and $\hat{\beta}^2_{ll,m} \triangleq \frac{p_p \tau_p \beta^2_{ll,m}}{\tau_p p_p \beta_{ll,m}+1}$, where p_p is the pilot power. The variances of $\tilde{\mathbf{h}}_{l,n}$ and $\tilde{\mathbf{g}}_{ll,m}$ are $\tilde{\beta}^2_{l,n} \triangleq \beta_{l,n} - \hat{\beta}^2_{l,n}$ and $\tilde{\beta}^2_{ll,m} \triangleq \beta_{ll,m} - \hat{\beta}^2_{ll,m}$, respectively.

B. Data Transmission Phase

Let $\mathbf{x}^s = [(\mathbf{x}^s_1)^T, (\mathbf{x}^s_2)^T, \cdots, (\mathbf{x}^s_K)^T]^T \in \mathbb{C}^{KN_S}$ denote the transmit signal from all the UEs, where $\mathbf{x}^s_l = [x^s_{l,1}, x^s_{l,2}, \cdots, x^s_{l,N_S}]^T \in \mathbb{C}^{N_S}$. Similarly, we let $\mathbf{x}^b = [(\mathbf{x}^b_1)^T, (\mathbf{x}^b_2)^T, \cdots, (\mathbf{x}^b_K)^T]^T \in \mathbb{C}^{KM_S}$ denote the BS transmit signals, where $\mathbf{x}^b_l = [x^b_{l,1}, x^b_{l,2}, \cdots, x^b_{l,M_S}]^T$. All K UEs transmit their signals to the BS in the UL. Simultaneously, the BS sends the intended data to each UE in the DL. The received signal $\mathbf{y}^b \in \mathbb{C}^{KN_S}$ at the BS and the l-th UE $\mathbf{y}^s_l \in \mathbb{C}^{M_S}$ are given, respectively, as

$$\mathbf{y}^b = \sqrt{p^s}\mathbf{W}^b\mathbf{H}\mathbf{x}^s + \sqrt{p^b}\mathbf{W}^b\mathbf{L}^b\mathbf{x}^b + \mathbf{W}^b\mathbf{n}^b, \tag{1}$$

$$\mathbf{y}^s_l = \mathbf{W}^s_l\Big[\sqrt{p^b}\mathbf{G}_{ll}\mathbf{x}^b_l + \sqrt{p^s}\sum\nolimits_{k' \neq l}^{K}\mathbf{G}_{lk'}\mathbf{x}^s_{k'} + \sqrt{p^s}\mathbf{C}^s_{ll}\mathbf{x}^s_l + \sqrt{p^s}\sum\nolimits_{k' \neq l}^{K}\mathbf{C}^s_{lk'}\mathbf{x}^s_{k'} + \mathbf{n}^s_l\Big], \tag{2}$$

where $\mathbf{W}^b \in \mathbb{C}^{KN_S \times M_R}$ and $\mathbf{W}^s_l \in \mathbb{C}^{M_S \times N_R}$ denote the receive filters at the BS and the l-th UE, respectively. p^s and p^b indicate the UE and BS transmit powers, respectively. $\mathbf{n}^s_l \in \mathbb{C}^{N_R}$ and $\mathbf{n}^b \in \mathbb{C}^{M_R}$ represent the noise vectors at the l-th UE and the BS, respectively. The elements of $\mathbf{x}^s$, $\mathbf{x}^b$, $\mathbf{n}^s_l$, and $\mathbf{n}^b$ are distributed by $\mathcal{CN}(0,1)$. $\mathbf{L}^b \in \mathbb{C}^{M_R \times KM_S}$ and $\mathbf{C}^s_{ll} \in \mathbb{C}^{N_R \times N_S}$ describe the residual SI channel matrix (after SI cancellation) at the BS and the l-th UE whose elements are modeled as $\mathcal{CN}(0, \sigma^2_m)$ and $\mathcal{CN}(0, \sigma^2_{ll})$, respectively. σ^2_m and σ^2_{ll} indicate the SI levels, which depend on the cancellation technique and the distance between the transmit and receive antenna arrays. $\mathbf{C}^s_{lk'} \in \mathbb{C}^{N_R \times (K-1)N_S}$ indicates the UE-to-UE interference channel. The elements of $\mathbf{C}^s_{lk'}$ are modeled as i.i.d. $\mathcal{CN}(0, \sigma^2_{lk'})$ random variables. The residual SI channels are modeled as Rayleigh fading, which is a common assumption in existing literature [2]. This assumption holds as the line-of-sight (LOS) components can be efficiently suppressed due to the cancellation mechanisms used, surrounding obstacles and the natural isolation provided by proper antenna separation [2], [7], [13].

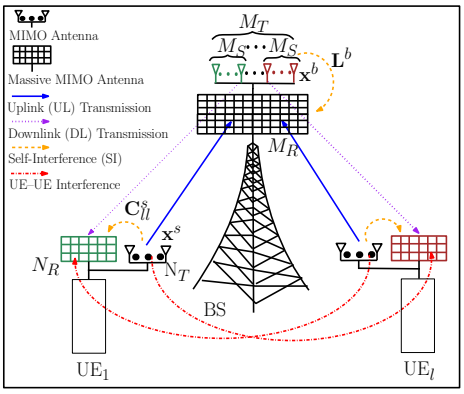

Fig. 1. Massive MIMO system with FD BS and FD UEs.

C. Signal Detection

The receive filters $\mathbf{W}^b \in \mathbb{C}^{KN_S \times M_R}$ at the BS and $\mathbf{W}^s_l \in \mathbb{C}^{M_S \times N_R}$ at the l-th UE are, respectively, given by

$$\mathbf{W}^b = \begin{cases} (\hat{\mathbf{H}}^H\hat{\mathbf{H}})^{-1}\hat{\mathbf{H}}^H, & \text{for ZF,} \\ \hat{\mathbf{H}}^H, & \text{for MRC.} \end{cases} \tag{3}$$

$$\mathbf{W}^s_l = \begin{cases} [(\hat{\mathbf{G}}^H_l\hat{\mathbf{G}}_l)^{-1}\hat{\mathbf{G}}^H_l]_j, & \text{for ZF,} \\ \hat{\mathbf{G}}^H_{ll}, & \text{for MRC,} \end{cases} \tag{4}$$

where j indicates the $[(l-1)M_S + 1 : lM_S]$ row. We discuss the achievable rate in the next section.

III. Achievable Rate Analysis

In this section, we analyze the sum-rate of the mMIMO system. To gain insights into the performance, the closed-form expressions for the achievable rate are derived by utilizing the approach in [3], where the received signal is written as a product of a known mean gain and the desired symbol plus an uncorrelated effective noise. The n-th stream of the received signals in (1) at the BS can be rewritten as:

$$y^b_{l,n} = \underbrace{\sqrt{p^s}\mathbb{E}\{\mathbf{w}^b_{l,n}\mathbf{h}_{l,n}\}x^s_{l,n}}_{\text{desired signal}} + \underbrace{\acute{n}^b}_{\text{effective noise}}, \tag{5}$$

$$\acute{n}^b \triangleq \underbrace{\sqrt{p^s}\left(\mathbf{w}^b_{l,n}\mathbf{h}_{l,n} - \mathbb{E}\{\mathbf{w}^b_{l,n}\mathbf{h}_{l,n}\}\right)x^s_{l,n}}_{\text{Gain error}} + \underbrace{\sqrt{p^s}\sum\nolimits_{n' \neq n}^{N_S}\mathbf{w}^b_{l,n}\mathbf{h}_{l,n'}x^s_{l,n'}}_{\text{Multi-stream interference from the } l\text{-th UE}} + \underbrace{\sqrt{p^b}\mathbf{w}^b_{l,n}\mathbf{L}^b\mathbf{x}^b}_{\text{BS SI}}$$
$$+ \underbrace{\sqrt{p^s}\sum_{k' \neq l}^{K}\sum_{n'=1}^{N_S}\mathbf{w}^b_{l,n}\mathbf{h}_{k',n'}x^s_{k',n'}}_{\text{Multi-UE Interference}} + \underbrace{\mathbf{w}^b_{l,n}\mathbf{n}^b}_{\text{Noise at the BS}}, \tag{6}$$

[3]Similar results is obtained if training is done as in [13]. To ensure mutually orthogonal pilots and avoid pilot contamination, we set $\tau_p \geq (N_S + M_S)K$.

where $\mathbf{w}_{l,n}^b \in \mathbb{C}^{M_R}$ is the $[(l-1)N_S+n]$-th row of $\mathbf{W}^b$.

Similarly, the m-th stream of the BS for the l-th UE signal is given by

$$y_{l,m}^s = \underbrace{\sqrt{p^b}\mathbb{E}\{\mathbf{w}_{l,m}^s \mathbf{g}_{ll,m}\}x_{l,m}^b}_{\text{desired signal}} + \underbrace{\acute{n}_l^s}_{\text{effective noise}}, \tag{7}$$

$$\begin{aligned}\acute{n}_l^s \triangleq\ & \underbrace{\sqrt{p^b}\left(\mathbf{w}_{l,m}^s \mathbf{g}_{ll,m} - \mathbb{E}\{\mathbf{w}_{l,m}^s \mathbf{g}_{ll,m}\}\right)x_{l,m}^b}_{\text{Gain error}} \\ & + \underbrace{\sqrt{p^b}\sum\nolimits_{m'\neq m}^{M_S} \mathbf{w}_{l,m}^s \mathbf{g}_{ll,m'} x_{l,m'}^b}_{\text{Multi-stream interference at BS}} + \underbrace{\mathbf{w}_{l,m}^s \mathbf{n}_l^s}_{\text{Noise at } l\text{-th UE}} \\ & + \underbrace{\sqrt{p^b}\sum\nolimits_{k'\neq l}^{K}\sum\nolimits_{m'=1}^{M_S} \mathbf{w}_{l,m}^s \mathbf{g}_{lk',m'} x_{k',m'}^b}_{\text{Interference from other BS antennas}} \\ & + \underbrace{\sqrt{p^s}\mathbf{w}_{l,m}^s \mathbf{C}_{ll}^s \mathbf{x}_l^s}_{l\text{-th UE SI}} + \underbrace{\sqrt{p^s}\sum\nolimits_{k'\neq l}^{K} \mathbf{w}_{l,m}^s \mathbf{C}_{lk'}^s \mathbf{x}_{k'}^s}_{\text{UE-to-UE interference}},\end{aligned} \tag{8}$$

where $\mathbf{w}_{l,m}^s \in \mathbb{C}^{N_R}$ is the m-th row of $\mathbf{W}_l^s$ and $\mathbf{g}_{lk',m'}$ represents the m'-th column of $\mathbf{G}_{lk'}$, $\forall m' = 1, \cdots, M_S$. Using (5), the achievable UL rate for the n-th stream of the l-th UE received at the BS is given by

$$R_{l,n}^{b,i} = \log_2\left(1 + \frac{A_{l,n}^b}{B_{l,n}^b + C_{l,n}^b + D_{l,n}^b + E_{l,n}^b + F_{l,n}^b}\right), \tag{9}$$

where $A_{l,n}^b = p^s|\mathbb{E}\{\mathbf{w}_{l,n}^b \mathbf{h}_{l,n}\}|^2$,
$B_{l,n}^b = p^s \mathbb{V}\text{ar}(\mathbf{w}_{l,n}^b \mathbf{h}_{l,n})$, $C_{l,n}^b = p^s \sum_{n'\neq n}^{N_S} \mathbb{E}\{|\mathbf{w}_{l,n}^b \mathbf{h}_{l,n'}|^2\}$,
$D_{l,n}^b = p^s \sum_{k'\neq l}^{K}\sum_{n'=1}^{N_S} \mathbb{E}\{|\mathbf{w}_{l,n}^b \mathbf{h}_{k',n'}|^2\}$,
$E_{l,n}^b = p^b\mathbb{E}\{|\mathbf{w}_{l,n}^b \mathbf{L}^b|^2\}$, and $F_{l,n}^b = \mathbb{E}\{|\mathbf{w}_{l,n}^b \mathbf{n}^b|^2\}$ represent the power of the desired signal, gain error, multi-stream interference from the l-th UE, multi-UE interference, SI, and the noise at the BS, respectively and $i \in \{\text{MRC, ZF}\}$.

Similarly, the achievable DL rate of the m-th data stream of the BS for the l-th UE is

$$R_{l,m}^{s,i} = \log_2\left(1 + \frac{A_{l,m}^s}{B_{l,m}^s + C_{l,m}^s + D_{l,m}^s + E_{l,m}^s}\right), \tag{10}$$

where $A_{l,m}^s = p^b|\mathbb{E}\{\mathbf{w}_{l,m}^s \mathbf{g}_{ll,m}\}|^2$, $B_{l,m}^s = p^b \mathbb{V}\text{ar}(\mathbf{w}_{l,m}^s \mathbf{g}_{ll,m})$,
$C_{l,m}^s = p^b \sum_{m'\neq m}^{M_S} \mathbb{E}\{|\mathbf{w}_{l,m}^s \mathbf{g}_{ll,m'}|^2\}$,
$D_{l,m}^s = p^b \sum_{k'\neq l}^{K}\sum_{m'=1}^{M_S} \mathbb{E}\{|\mathbf{w}_{l,m}^s \mathbf{g}_{lk'm'}|^2\}$, and
$E_{l,m}^s = p^s\mathbb{E}\{|\mathbf{w}_{l,m}^s \mathbf{C}_{ll}^s|^2\} + p^s \sum_{k'\neq l}^{K} \mathbb{E}\{|\mathbf{w}_{l,m}^s \mathbf{C}_{lk'}^s|^2\}$
$+\mathbb{E}\{|\mathbf{w}_{l,m}^s \mathbf{n}_l^s|^2\}$ represent the power of the desired signal, gain error, BS multi-stream interference, interference from other BS antennas, and the sum of the power of the l-th UE SI, UE-to-UE interference, and the noise at the l-th UE, respectively.

A. Closed-form solutions based on ZF and MRC

Here, we evaluate the closed-form solutions using ZF and MRC.

Theorem 1. *In the presence of imperfect CSI, the achievable UL rate for the n-th stream of the l-th UE at the BS and the DL achievable rate for the m-th data stream of the BS for the l-th UE of the FD massive MIMO system using ZF are, respectively, given by*

$$R_{l,n}^{b,ZF} = \log_2\left(1 + \frac{p^s(M_R - KN_S)\hat{\beta}_{l,n}^2}{p^s\sum_{k'=1}^{K}\sum_{n'=1}^{N_S}\tilde{\beta}_{k',n'}^2 + \zeta + 1}\right), \tag{11}$$

$$R_{l,m}^{s,ZF} = \log_2\left(1 + \frac{p^b(N_R - KM_S)\hat{\beta}_{ll,m}^2}{p^b\sum\limits_{k'=1}^{K}\sum\limits_{m'=1}^{M_S}\tilde{\beta}_{lk',m'}^2 + \Psi + 1}\right), \tag{12}$$

where $\Psi = p^s(\sigma_{ll}^2 + \sum_{k'\neq l}^{K}\sigma_{lk'}^2)N_S$ and $\zeta = p^b\sigma_m^2 KM_S$.

Proof. Please refer to Appendix A. □

The numerators in (11) and (12) indicate the beamforming gains in the UL and DL, respectively. Increasing M_R and N_R antennas causes a monotonic increase in the achievable rate. However, there is a decrease of KN_S and KM_S DoF in the beamforming gains in the UL and DL, respectively, to place the signals in a null space and suppress interference. The denominators in (11) and (12) constitute the power of the interferences and noise. The first term in denominators in (11) and (12), known as non-coherent interference (NCI), is independent of the receive antennas but depends on the mean-square of the channel estimation error. As the quality of the channel estimate improves, the NCI power decreases. It is observed from ζ in (11) that the BS SI depends on the BS transmit power, number of UEs, data streams transmitted by the BS, and the BS SI level. When these terms are fixed, decreasing BS transmit power can help reduce the BS SI at the expense of the DL rate. Also, as seen from Ψ in (12), the UE SI and UE-to-UE interference depend on the UE transmit power, the number of UEs, and the UE data streams. Similarly, reducing the transmit power at the UEs decreases the SI and consequently lowers the UL rate. The BS and UEs SI can also be reduced by increasing the number of receive antennas.

Theorem 2. *By using the MRC receiver and under the assumption of imperfect CSI, the achievable UL rate for the n-th data stream of the l-th UE at the BS and the achievable DL rate for the m-th stream of the BS for the l-th UE of the FD mMIMO system are expressed as*

$$R_{l,n}^{b,MRC} = \log_2\left(1 + \frac{p^s M_R \hat{\beta}_{l,n}^2}{p^s\sum_{k'=1}^{K}\sum_{n'=1}^{N_S}\beta_{k',n'} + \zeta + 1}\right), \tag{13}$$

$$R_{l,m}^{s,MRC} = \log_2\left(1 + \frac{p^b N_R \hat{\beta}_{ll,m}^2}{p^b\sum_{k'=1}^{K}\sum_{m'=1}^{M_S}\beta_{lk',m'} + \Psi + 1}\right), \tag{14}$$

respectively.

Proof. Please refer to Appendix B. □

The beamforming gains, i.e., the numerators of (13) and (14), grow proportionally with M_R and N_R, respectively. Unlike ZF, MRC does not sacrifice any DoF to reduce interference power. The NCI power, which depends on the channel gains in MRC, is thus more pronounced compared to ZF. ζ denotes the effect of the BS SI and Ψ represents the UE SI and the UE-to-UE interference powers. ζ and Ψ depend on the SI strength, transmit power, number of UEs and the number of streams. The effect of ζ and Ψ can be counteracted by increasing M_R and N_R.

Remark. *As the signal-to-noise ratio (SNR) $\triangleq p^s = p^b \longrightarrow \infty$ (assuming unit noise power),* (11)-(14) *reduce to* $\tilde{R}_{l,n}^{b,ZF} = \log_2\left(1 + \frac{(M_R - KN_S)\hat{\beta}_{l,n}^2}{\sum_{k'=1}^{K}\sum_{n'=1}^{N_S}\tilde{\beta}_{k',n'}^2 + \sigma_m^2 KM_S}\right)$,

This article has been accepted for publication in IEEE Transactions on Vehicular Technology. This is the author's version which has not been fully edited and content may change prior to final publication. Citation information: DOI 10.1109/TVT.2023.3266715

$$\tilde{R}_{l,m}^{s,ZF} = \log_2\left(1+\frac{(N_R-KM_S)\hat{\beta}_{ll,m}^2}{\sum_{k'=1}^{K}\sum_{m'=1}^{M_S}\tilde{\beta}_{lk',m'}^2+\bar{\Psi}}\right),$$

$$\tilde{R}_{l,n}^{b,MRC} = \log_2\left(1+\frac{M_R\hat{\beta}_{l,n}^2}{\sum_{k'=1}^{K}\sum_{n'=1}^{N_S}\beta_{k',n'}+\sigma_m^2KM_S}\right), \textit{ and}$$

$$\tilde{R}_{l,m}^{s,MRC} = \log_2\left(1+\frac{N_R\hat{\beta}_{ll,m}^2}{\sum_{k'=1}^{K}\sum_{m'=1}^{M_S}\beta_{lk',m'}+\bar{\Psi}}\right), \textit{ respectively,}$$

where $\bar{\Psi} = (\sigma_{ll}^2+\sum_{k'\neq l}^{K}\sigma_{lk'}^2)N_S$.

The transmit and interference powers grow simultaneously with the SNR. As such, the SE cannot be improved by merely increasing transmit power.

B. Sum SE

The sum SE of the system of the FD mMIMO system using ZF or MRC is expressed as $SE = \frac{T-\tau_p}{T}R^i$, where

$$R^i = \sum_{l=1}^{K}\left(\sum_{n=1}^{N_S}R_{l,n}^{b,i}+\sum_{m=1}^{M_S}R_{l,m}^{s,i}\right). \tag{15}$$

To obtain the optimal number of streams for maximum sum SE, a one-dimensional search method such as the golden-section search (GSS) algorithm is employed. GSS is known to minimize the number of iterations and improve the optimum SE convergence rate [14].

Algorithm 1 Optimal number of streams/pilot length line search algorithm

1: Initialize the number of streams
2: **repeat**
3: Calculate the sum SE
4: Update τ_p or streams[4] with a line search algorithm
5: **until** Convergence

IV. Numerical Results

In this section, numerical results are presented to corroborate the accuracy of the derived results. Unless otherwise stated, we assume that $\sigma_m^2 = \sigma_{ll}^2 = \sigma_{lk'}^2 = 0.3$, $\forall l$. The pilot power, coherence interval, and the pilot sequence length are $p_p = 10$ dB, $T = 200$ (symbols), and $\tau_p = K(M_S+N_S)$, respectively. We assume that the BS and UEs transmit equal number of data streams i.e., $M_S = N_S$. We set $\beta_{l,n} = \beta_{ll,m} = 0.1, \forall l$, $N_T = N_S$, $M_T = KM_S$. Monte-Carlo simulations are averaged over 10^4 channel realizations.

Fig. 2 shows the sum-rate versus the SNR. The simulation results are obtained by substituting (9)-(10) into (15) while the analytical results are obtained by placing (11)-(12) and (13)-(14) into (15) for ZF and MRC, respectively. It is observed that the analytical plots match tightly with the simulation. In Fig 2(a), due to better interference suppression, ZF outperforms MRC in the high SNR region for $K = 2, 4$. As the number of UEs increases from 2 to 4, the sum-rate improves due to increased multiplexing gain. However, as the SNR increases, the sum-rate saturates because the interference power also rises (see Remark). The effect of a few receive antennas on the sum-rate is demonstrated in Fig. 2(b). ZF performs worse than MRC with fewer antennas, as the available DoF for nulling interference in ZF is insufficient (see numerators (11)-(12)). However, as M_R (N_R) increases, ZF performs better than MRC as typically expected[5]. Overall, additional antennas improve the SE, but ZF provides about 2.29 bits/s/Hz gain over MRC as the effect of NCI power in ZF is further reduced compared to MRC (see denominators in (12)-(14)).

Next, we plot the sum SE against the SNR in Fig. 3(a). At SNR $= 5$ dB, there are about 10 bits/s/Hz and 9 bits/s/Hz

[4]Round off non-integer values of τ_p or streams to the nearest whole number.

[5]This also occurs in generic systems as well [1]. However, the configuration used here is a little different. Also we consider multi-stream effects.

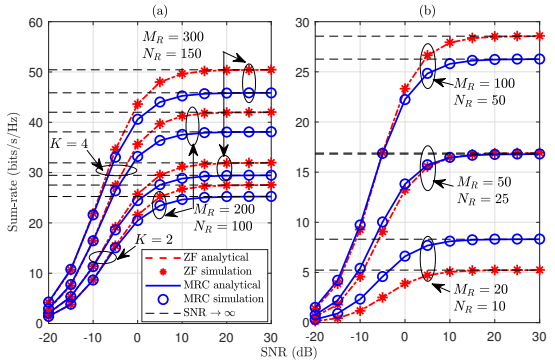

Fig. 2. Sum-rate versus SNR, where $p_p = 10$ dB, and $T = 200$. (a) $M_R = 300, 200$, $N_R = 150, 100$, $K = 2, 4$ (b) $M_R = 100, 50$, $N_R = 50, 25$, $K = 4$.

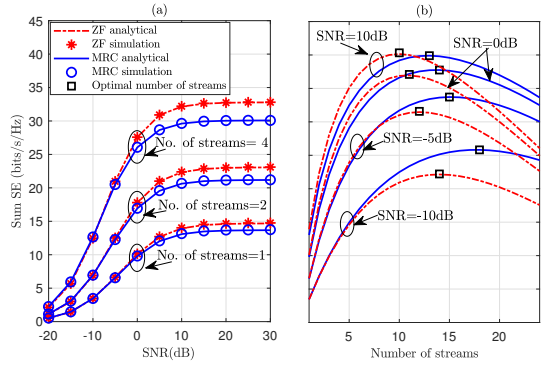

Fig. 3. (a) Sum SE versus SNR, where $M_R = 200$, $N_R = 50$, $K = 2$, $p_p = 10$ dB, $\sigma_{ll}^2 = 0.3$, and $T = 200$. (b) Sum SE against number of streams.

gains for ZF and MRC, respectively, as the number of streams increases from 2 to 4 ZF reduces multi-stream transmission effects and performs better than MRC, especially in the high SNR region. For example, at SNR $= 20$ dB, ZF has about 1.86 bits/s/Hz and 2.67 bits/s/Hz gain over MRC for 2 and 4 streams, respectively. However, the benefit of multi-stream transmission eventually wanes due to the corresponding rise in channel estimation overhead and multi-stream interference. This effect is shown in Fig. 3(b), where the sum SE is plotted against the number of streams for different SNR values. The sum SE initially increases with the number of streams and grows to an optimal point but finally declines due to increased interference (SI, UE-to-UE, and NCI). Here, ZF decays faster than MRC (see comments in Theorems (1) and (2)). The optimal number of streams shown with the black squares in Fig. 3(b) is found by using Algorithm 1. The sum SE also grows with the SNR due to improved beamforming. Increasing the SNR further slows down the SE growth as the interferences stated above depend on the transmit power. For example, with 8 data streams and a fixed number of antennas, the SE of MRC increases by 9.28 bits/s/Hz when the SNR increases from -10 dB to -5 dB and by about 2.89 bits/s/Hz when the SNR increases from 0 dB to 10 dB whereas the SE for ZF increases by 10.21 bits/s/Hz and 3.72 bits/s/Hz when the SNR rises from -10 dB to -5 dB and 0 dB to 10 dB, respectively.

The effect of the pilot length on the sum SE is investigated in Fig. 4. The sum SE increases with pilot length for MRC and ZF due to better channel estimation. However, as the pilot length increases, the available slot for data transmission reduces, causing the SE to decrease. Also, the pilot length required to achieve optimum sum SE reduces with increasing pilot power. As shown in Fig. 4, ZF attains slightly higher performance than MRC for any number of UEs and a few data streams e.g., 2 streams. The optimal pilot lengths (black circles) for the maximum SE are found with Algorithm 1. The effect of SI on sum SE when the BS and UEs operate

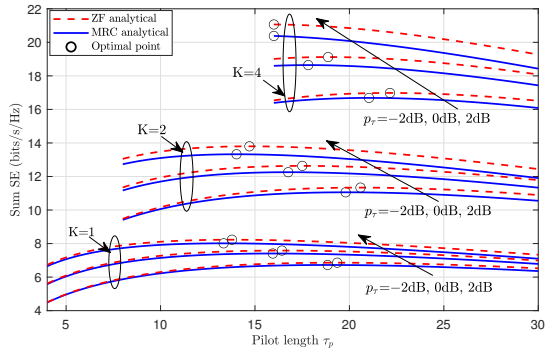

Fig. 4. Sum SE versus pilot length, where $N_S = M_S = 2$, $T = 100$, $M_R = 200$, and $N_R = 50$.

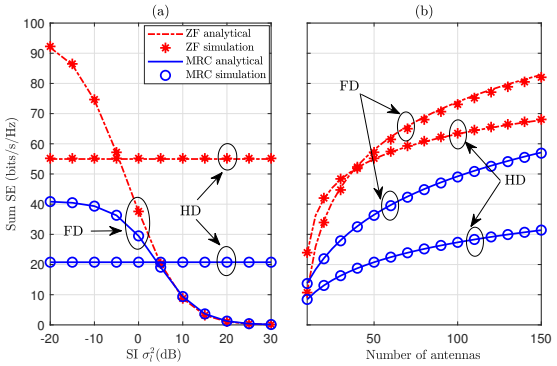

Fig. 5. (a) Sum SE versus SI, where $N_S = M_S = 2$, $K = 4$, $T = 200$, $M_R = N_R = 50$, and $p^s = p^b = p_p = 5$ dB. (b) Sum SE versus number of massive antennas, with $\sigma_{ll}^2 = -5$ dB.

in either HD or FD mode is shown in Fig. 5(a). In the HD mode, the sum SE is obtained by setting all the SI and UE-to-UE interference terms in (15) to zero. In addition, the HD mode imposes a prelog factor of half on the sum SE and uses double the transmit power of the FD system to ensure fairness. In Figs. 5(a) and 5(b), the parameters are set as: $p^s = p^b = 5$ dB, $\beta_{l,n} = \beta_{ll,m} = 1$, and $K = 4$. Due to the larger prelog factor of one, FD outperforms the HD mode under low SI regime as seen in Fig. 5(a). However, the SE of FD sharply declines as the SI increases and eventually dominates the system. Fig. 5(b) plots the sum SE against the number of antennas. A larger antenna array aids in combating SI as the system exploits the increased DoF offered by the number of antennas (spatial diversity) to mitigate overall interference. Similar to the previous plot in Fig. 5(a), FD offers an increased sum SE over HD due to the larger prelog factor.

V. Conclusion

This paper analyzed the performance of a mMIMO system where the FD BS and UEs with a large-antenna array transmit/receive multiple data streams. MRC and ZF schemes are employed to detect the signals. The results show that a few data streams are beneficial for increasing the SE. However, as the number of streams increases, multi-stream interference and estimation overhead reduce performance. Also, ZF performs better than MRC in the high SNR region.

Appendix A

Proof of Theorem 1: The desired signal power in (9) is given by $A_{l,n}^b = p^s|\mathbb{E}\{\mathbf{w}_{l,n}^b\mathbf{h}_{l,n}\}|^2 = p^s$. From the ZF matrix in (3), we can write $\mathbf{W}^b\mathbf{H} = \mathbf{I} + \mathbf{W}^b\tilde{\mathbf{H}}$ and $\mathbf{w}_{l,n}^b\mathbf{h}_{l,n} = 1 + \mathbf{w}_{l,n}^b\tilde{\mathbf{h}}_{l,n}$ since $\mathbf{w}_{l,n}^b$ and $\tilde{\mathbf{h}}_{l,n}$ are uncorrelated. The variance is given as $B_{l,n}^b = p^s\mathbb{V}\text{ar}(\mathbf{w}_{l,n}^b\mathbf{h}_{l,n})$ $= p^s\mathbb{E}\{|\mathbf{w}_{l,n}^b\mathbf{h}_{l,n}|^2\} - p^s\left(\mathbb{E}\{\mathbf{w}_{l,n}^b\mathbf{h}_{l,n}\}\right)^2 = \frac{p^s\tilde{\beta}_{l,n}^2}{(M_R - KN_S)\hat{\beta}_{l,n}^2}$. The multi-stream interference power from the l-th UE, $C_{l,n}^b = p^s\sum_{n'\neq n}^{N_S}\mathbb{E}\{|\mathbf{w}_{l,n}^b\mathbf{h}_{l,n'}|^2 = p^s\sum_{n'\neq n}^{N_S}\mathbb{E}\{|\mathbf{w}_{l,n}^b\tilde{\mathbf{h}}_{l,n'}|^2\} = p^s\sum_{n'\neq n}^{N_S}\frac{\tilde{\beta}_{l,n'}^2}{(M_R - KN_S)\hat{\beta}_{l,n}^2}$. Also, the multi-UE interference power $D_{l,n}^b = p^s\sum_{k'\neq l}^{K}\sum_{n'=1}^{N_S}\mathbb{E}\{|\mathbf{w}_{l,n}^b\mathbf{h}_{k',n'}|^2\} = p^s\sum_{k'\neq l}^{K}\sum_{n'=1}^{N_S}\frac{\tilde{\beta}_{k',n'}^2}{(M_R - KN_S)\hat{\beta}_{l,n}^2}$. The BS SI power is obtained as $E_{l,n}^b = p^b\mathbb{E}\{|\mathbf{w}_{l,n}^b\mathbf{L}^b|^2\} = \frac{p^b\sigma_m^2 KM_S}{(M_R - KN_S)\hat{\beta}_{l,n}^2}$. The BS noise power $F_{l,n}^b = \mathbb{E}\{|\mathbf{w}_{l,n}^b\mathbf{n}^b|^2\} = \frac{1}{(M_R - KN_S)\hat{\beta}_{l,n}^2}$. By plugging these terms into (9), (11) is obtained. Similarly, (12) can be obtained using the above steps.

Appendix B

Proof of Theorem 2: Following similar steps used for [15, (19)] and [3, (6)], the desired signal power is given as $A_{l,n}^b = p^s|\mathbb{E}\{\mathbf{w}_{l,n}^b\mathbf{h}_{l,n}\}|^2 = p^s|\mathbb{E}\{\hat{\mathbf{h}}_{l,n}^H\mathbf{h}_{l,n}\}|^2 = p^s{M_R}^2(\hat{\beta}_{l,n}^2)^2$. The variance $B_{l,n}^b = p^s\mathbb{V}\text{ar}(\mathbf{w}_{l,n}^b\mathbf{h}_{l,n}) = p^sM_R\beta_{l,n}\hat{\beta}_{l,n}^2$. For the multi-stream interference power from the l-th UE, we obtain $C_{l,n}^b = p^s\sum_{n'\neq n}^{N_S}\mathbb{E}\{|\mathbf{w}_{l,n}^b\mathbf{h}_{l,n'}|^2\} = p^s\mathbb{E}\{|\hat{\mathbf{h}}_{l,n}^H(\hat{\mathbf{h}}_{l,n'} + \tilde{\mathbf{h}}_{l,n'}\}|^2\} = p^sM_R\beta_{l,n'}\hat{\beta}_{l,n}^2$. The multi-UE interference power $D_{l,n}^b = p^s\sum_{k'\neq l}^{K}\sum_{n'=1}^{N_S}\mathbb{E}\{|\mathbf{w}_{l,n}^b\mathbf{h}_{k',n'}|^2\} = p^sM_R\beta_{k',n'}\hat{\beta}_{l,n}^2$. The BS SI power, $E_{l,n}^b = p^b\mathbb{E}\{|\mathbf{w}_{l,n}^b\mathbf{L}^b|^2\} = p^b\sigma_m^2KM_SM_R\hat{\beta}_{l,n}^2$. The noise at BS is given by $F_{l,n}^b = \mathbb{E}\{|\mathbf{w}_{l,n}^b\mathbf{n}^b|^2\} = M_R\hat{\beta}_{l,n}^2$. Substituting these terms into (9), (13) is obtained. Please note that (14) is also found with the above steps.

References

[1] H. Q. Ngo, E. G. Larsson, and T. L. Marzetta, "Energy and spectral efficiency of very large multiuser MIMO systems," *IEEE Trans. Commun.*, vol. 61, pp. 1436–1449, Apr. 2013.

[2] P. Anokye *et al.*, "Achievable sum-rate analysis of massive MIMO full-duplex wireless backhaul links in heterogeneous cellular networks," *IEEE Access*, vol. 6, pp. 23456–23469, Apr. 2018.

[3] B. D. Antwi-Boasiako *et al.*, "On the performance of massive MIMO full-duplex relaying with low-resolution ADCs," *IEEE Commun. Lett.*, vol. 26, pp. 1259–1263, Jun. 2022.

[4] X. Li, E. Björnson, S. Zhou, and J. Wang, "Massive MIMO with multi-antenna users: When are additional user antennas beneficial?," in *Proc. 23rd Int. Conf. Telecommun. (ICT)*, pp. 1–6, May 2016.

[5] H. Q. Ngo *et al.*, "Massive MU-MIMO downlink TDD systems with linear precoding and downlink pilots," in *Proc. 51st Annu. Allerton Conf. Commun. Control Comput. (Allerton)*, pp. 293–298, Oct. 2013.

[6] W. Hong, K.-H. Baek, Y. Lee, Y. Kim, and S.-T. Ko, "Study and prototyping of practically large-scale mmWave antenna systems for 5G cellular devices," *IEEE Commun. Mag.*, vol. 52, pp. 63–69, Sept. 2014.

[7] J. Feng, S. Ma, G. Yang, and H. V. Poor, "Impact of antenna correlation on full-duplex two-way massive MIMO relaying systems," *IEEE Trans. Wireless Commun.*, vol. 17, pp. 3572–3587, June 2018.

[8] A. Shojaeifard *et al.*, "Massive MIMO-enabled full-duplex cellular networks," *IEEE Trans. Commun.*, vol. 65, pp. 4734–4750, Nov. 2017.

[9] P. Zhu, Z. Sheng, J. Bao, and J. Li, "Antenna selection for full-duplex distributed massive MIMO via the elite preservation genetic algorithm," *IEEE Commun. Lett.*, vol. 26, no. 4, pp. 922–926, 2022.

[10] K. Min *et al.*, "Antenna ratio for sum-rate maximization in full-duplex large-array base station with half-duplex multiantenna users," *IEEE Trans. Veh. Technol*, vol. 65, pp. 10168–10173, Dec. 2016.

[11] A. Ashikhmin, L. Li, and T. L. Marzetta, "Interference reduction in multi-cell massive MIMO systems with large-scale fading precoding," *IEEE Trans. Inf. Theory*, vol. 64, pp. 6340–6361, Sept. 2018.

[12] B. Li, D. Zhu, and P. Liang, "Small cell in-band wireless backhaul in massive MIMO systems: A cooperation of next-generation techniques," *IEEE Trans. Wireless Commun.*, vol. 14, pp. 7057–7069, Dec. 2015.

[13] C. Kong, C. Zhong, S. Jin, S. Yang, H. Lin, and Z. Zhang, "Full-duplex massive MIMO relaying systems with low-resolution ADCs," *IEEE Trans. Wireless Commun.*, vol. 16, pp. 5033–5047, Aug. 2017.

[14] J. Zeng *et al.*, "Enabling ultrareliable and low-latency communications under shadow fading by massive MU-MIMO," *IEEE Internet Things J.*, vol. 7, pp. 234–246, Jan. 2020.

[15] X. Hu, C. Zhong, X. Chen, W. Xu, H. Lin, and Z. Zhang, "Cell-free massive MIMO systems with low resolution ADCs," *IEEE Trans. on Commun.*, vol. 67, pp. 6844–6857, Oct. 2019.